

Electronic structure of the Ni-Pd-P and Ni-Pt-P metallic glasses: A pulsed NMR study

W. A. Hines,* K. Glover, and W. G. Clark

*Department of Physics, University of California at Los Angeles,
Los Angeles, California 90024*

L. T. Kabacoff† and C. U. Modzelewski

*Department of Physics and Institute of Materials Science,
University of Connecticut, Storrs, Connecticut 06268*

R. Hasegawa

Materials Research Center, Allied Chemical Corporation, Morristown, New Jersey 07960

P. Duwez

*W. M. Keck Laboratory of Engineering Materials, California Institute of Technology,
Pasadena, California 91109*

(Received 11 December 1979)

A pulsed NMR and magnetic susceptibility study of the electronic structure is reported for the rapidly quenched metallic glass systems: $(\text{Ni}_{0.50}\text{Pd}_{0.50})_{100-x}\text{P}_x$ (where $16 \leq x \leq 26.5$), $(\text{Ni}_y\text{Pd}_{1-y})_{80}\text{P}_{20}$ (where $0.20 \leq y \leq 0.80$), and $(\text{Ni}_y\text{Pt}_{1-y})_{75}\text{P}_{25}$ (where $0.20 \leq y \leq 0.69$). The ^{31}P Knight shift and nuclear spin-lattice relaxation rate in all three systems depend only on the P concentration, x , and not the Ni concentration, y , nor whether the second transition metal is Pd or Pt. Both the shift and relaxation rate for ^{31}P are attributed solely to the direct contact hyperfine interaction. The ^{195}Pt Knight shift and magnetic susceptibility for $(\text{Ni}_y\text{Pt}_{1-y})_{75}\text{P}_{25}$ do depend on both the Ni concentration and temperature, enabling a determination of the contributions to the shift arising from the direct contact hyperfine and core polarization interactions. The results are discussed in terms of a rigid two-band picture with estimates being made for the s - and d -band densities of states and hyperfine coupling constants. There is strong evidence for a transfer of charge from the P metalloid atoms (M) to the d states of the transition-metal atoms (T), which is consistent with the dense random packing model for $T_{100-x}M_x$ metallic glasses.

I. INTRODUCTION

During the past few years, considerable research effort has been devoted to a class of materials known as "amorphous metallic alloys" or "metallic glasses", i.e., solids which have the electrical properties normally associated with metals, but are not spatially periodic.¹ This is due to a desire for a reexamination of some fundamental concepts of solids as well as possibilities for technological application. One general family of metallic glasses has the characteristic form $T_{100-x}M_x$, where T is a transition metal (or combination of transition metals) such as Ni, Pd, Pt, or Fe, and M is a high-valence metalloid (or combination of metalloids) such as B, C, Si, or P. Typically, such alloys are prepared by rapid quenching from the liquid state and possess metalloid compositions ranging from $x = 15$ to 30 at. %.

This work describes the application of pulsed nuclear magnetic resonance (NMR) techniques, supple-

mented by magnetic susceptibility measurements, in the study of the electronic structure for several Ni-Pd-P and Ni-Pt-P metallic glasses. The consequences of such an investigation are many fold in that a knowledge of their electronic structure leads to a better understanding of the electrical, magnetic, and mechanical properties for metallic glasses in general. These systems were selected because they are easily prepared in the glassy state with considerable variation in the metalloid concentration as well as the relative transition-metal composition. In addition, the metalloid ^{31}P and transition metal ^{195}Pt are excellent candidates for NMR.

The Ni-Pd-P and Ni-Pt-P systems have been studied by x-ray diffraction,²⁻⁴ resulting in a knowledge of their radial distribution functions (RDF). Also, measurements of the electrical resistivity,^{5,6} thermopower,⁶ glass transition temperature,⁷ and crystallization temperature⁷ have been carried out. In an earlier work,⁸ we reported NMR results in which mea-

surements of the ^{31}P Knight shift and linewidth were obtained through steady-state techniques. These results provided a qualitative description of the electronic and glassy atomic structure. By incorporating the earlier steady-state NMR work with the pulsed NMR and magnetic susceptibility results reported here, we obtain a clearer picture of the nature of the electronic structure in metallic glasses, along with quantitative estimates for the *s*- and *d*-band densities of states and hyperfine coupling constants.

In any discussion of the electronic structure for $T_{100-x}M_x$ metallic glasses, a knowledge of the atomic structure is of prime importance. Several models have been proposed. One of the most widely used models for the structure of metallic glass systems in which the constituent transition metal and metalloid atoms have similar atomic size is that suggested by Polk.⁹ In this model, a hard-sphere dense random packing (DRP) structure is postulated for the transition-metal atoms which is similar to that proposed for liquid metals by Bernal.¹⁰ The metalloid atoms occupy the larger (interstitial) holes inherent in such a structure and, hence, are always surrounded by transition-metal atoms as first nearest neighbors. This simple model has several attractive features and is in both qualitative and quantitative agreement with many experiments. Early calculations of the RDF from such a model were in very good agreement with those obtained by x-ray-diffraction measurements. (Also, we note that if the atomic sizes of the constituents are taken into account, the RDF for all the $T_{100-x}M_x$ metallic glasses are essentially alike, implying a great deal of similarity in their glassy atomic structures.) Recently, however, more detailed structural studies have resulted in some criticism of this model. As pointed out by Nagel,¹¹ there is an apparent discrepancy concerning the coordination number of the metalloid atoms which can only be resolved by assuming some distortion in the Bernal structure as well as having one type of hole predominate. Even with its flaws, the DRP model does serve as a reasonable first approximation in describing the structure of these materials. The main competitor to the DRP model is the microcrystalline model.¹² In this model, the metallic glass is treated as a polycrystalline material with vanishingly small grain size. Due to line broadening effects, x-ray-diffraction techniques cannot totally eliminate the possibility of crystallites with dimensions $\leq 15 \text{ \AA}$.

Three general descriptions for the nature of the electronic structure in metallic glasses have been presented, with the particular goal of explaining bonding, structural stability, and glass-forming tendency. The first is based on the dense random packing structure described above. In the DRP model, Polk⁹ suggests that a transfer of charge from the metalloids to the *d* states of the transition-metal atoms takes place which results in a form of ionic-

like bonding that stabilizes the structure. This model has had some success, particularly in predicting the range of metalloid composition. However, Chen¹³ has raised objections to such an explanation because of his studies concerning the stability, radial distribution function, and atomic size characteristics of several metallic glass systems. He suggests that there is strong chemical (or covalent) bonding between the metalloid and transition-metal atoms; and, that short-range order persists in the liquid state near the glass-forming composition. From this point of view, we might expect the atomic structure to have a short-range order similar to the crystalline state, but no long-range order. X-ray and ultraviolet photoemission measurements of the core levels and valence bands of crystalline Pd, and of both crystalline and glassy $\text{Pd}_{77.5}\text{Cu}_{6.0}\text{Si}_{16.5}$, have been carried out by Nagel *et al.*¹⁴ Their results gave no evidence of any significant chemical bonding contribution to the glass-forming tendency or stability against crystallization for this alloy. However, they do concede the possibility of bonding effects which do not appreciably affect the core levels and thus, would have gone undetected by the photoemission experiments. A third model, based on the nearly free-electron approach, has been proposed by Nagel and Tauc.¹⁵ They suggest that the alloy is most stable when the composition is such that the Fermi level lies at a minimum in the density of electronic states. This nearly free-electron model, which employs many of the concepts from Ziman's¹⁶ theory of liquid metals, gains support from measurements of the electrical resistivity and glass transition temperature, and also predicts the correct composition range. Of critical importance in this model is the relationship between $2k_F$ and k_p , where k_F is the Fermi wave vector and k_p is the value of the wave vector corresponding to the first peak in the structure factor $a(k)$. Typically, $2k_F \approx k_p$ when the average electron to atom ratio is 1.7, and it is under this condition that the Fermi energy lies at the minimum in the density of states. Also, the larger $a(k_p)$, the deeper will be the minimum and, hence, the more stable will be the alloy. Since metallic glasses are generally transition-metal based alloys, the application of liquid metal theories such as Ziman's pseudopotential approach is open to question. We note, however, that Evans *et al.*¹⁷ have extended the liquid theory to include transition-metal alloys by replacing the pseudopotential of the Ziman nearly free-electron approach with the *t* matrix of a muffin-tin potential. Finally, the general question concerning the application of certain rigid-band ideas to metallic glasses has recently been discussed by Cote.¹⁸ He suggests that a "sinking-band" model (similar to that proposed by Beebe¹⁹ for crystalline transition-metal based alloys) is a far better description of metallic glasses than the usual rigid-band model.

II. EXPERIMENTAL APPARATUS AND PROCEDURE

A. Sample preparation

In this work, pulsed NMR and magnetic susceptibility experiments were carried out on the following metallic glass systems: $(\text{Ni}_{0.50}\text{Pd}_{0.50})_{100-x}\text{P}_x$ (where $x = 16, 16.6, 17, 20, 23, 25,$ and 26.5), $(\text{Ni}_y\text{Pd}_{1-y})_{80}\text{P}_{20}$ (where $y = 0.20, 0.30, 0.40, 0.50, 0.60, 0.70,$ and 0.80) and $(\text{Ni}_y\text{Pt}_{1-y})_{75}\text{P}_{25}$ (where $y = 0.20, 0.30, 0.40, 0.50, 0.60, 0.64,$ and 0.68). All of the alloys were prepared by a rapid quenching process (piston and anvil technique) described in detail elsewhere.²⁰ The foils which resulted from the process were about $50 \mu\text{m}$ thick and 2.5 cm in diameter, and were checked by x-ray diffraction to verify their glassy structure. In order to obtain a good filling factor for the NMR experiments, the foils were cut and stacked with alternate layers of $12\text{-}\mu\text{m}$ Mylar.

B. Nuclear magnetic resonance

The variable-frequency pulsed NMR apparatus and single-coil arrangement are similar to those described elsewhere.²¹ A conventional double Dewar system enabled operation at liquid helium and nitrogen temperatures. Measurements of the nuclear spin-lattice relaxation rate, $1/T_1$, were made by employing a $\frac{1}{2}\pi - \frac{1}{2}\pi$ pulse sequence, while Knight-shift, K , measurements were obtained by using a single $\frac{1}{2}\pi$ pulse and sweeping the magnetic field through the resonance with a conventional "boxcar" to obtain the absorption signal by integrating the free-induction decay.²¹ The magnetic field sweep was calibrated with a marginal oscillator which monitored the ^2D resonance ($\gamma = 0.653566 \text{ kHz/Oe}$).²² For calculating the ^{31}P and ^{195}Pt Knight shifts, values of $\gamma = 1.7236_0 \text{ kHz/Oe}$ and 0.9153_0 kHz/Oe were used for the ^{31}P and ^{195}Pt salt references, respectively.²²

C. Magnetic susceptibility

All measurements of the magnetic susceptibility were carried out on a P.A.R. model 155 vibrating sample magnetometer (Foner method²³). Temperatures ranging continuously from 3 K to room temperature were obtainable with the Janis model 153 "Super Varitemp" Dewar accessory, while magnetic fields up to 20 kOe were also available. The magnetometer was calibrated against the known saturation magnetization for Ni (room-temperature value of 55.01 emu/g). The low-temperature calibration was based on the ideal Curie-Weiss behavior of the paramagnetic salt $\text{Gd}_2(\text{SO}_4)_3 \cdot 8\text{H}_2\text{O}$. For all of the samples, plots of the bulk magnetization (per mole) versus field yielded straight lines that passed through the origin indicating no significant ferromagnetic contamination. Values of the magnetic susceptibility at 77 K and room temperature were calculated from the corresponding slopes.

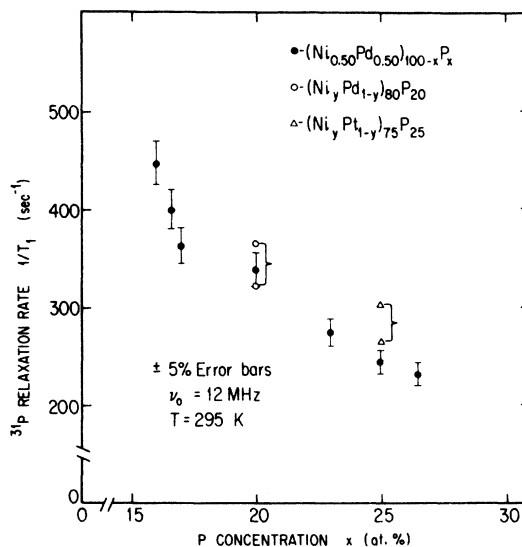


FIG. 1. Room-temperature ^{31}P nuclear spin-lattice relaxation rate vs P concentration for the $(\text{Ni}_{0.50}\text{Pd}_{0.50})_{100-x}\text{P}_x$ system: solid circles. The two open circles with bracket represent the range of values for $(\text{Ni}_y\text{Pd}_{1-y})_{80}\text{P}_{20}$, while the two open triangles with bracket represent the range of values for $(\text{Ni}_y\text{Pt}_{1-y})_{75}\text{P}_{25}$. $1/T_1$ for ^{31}P depends only on the metalloid concentration and not on the relative transition-metal composition for these systems.

III. EXPERIMENTAL RESULTS

A. ^{31}P NMR spin-lattice relaxation rate

Figure 1 shows the observed room temperature ^{31}P nuclear spin-lattice relaxation rate (in sec^{-1}), $1/T_1$, as a function of P concentration, x , for the $(\text{Ni}_{0.50}\text{Pd}_{0.50})_{100-x}\text{P}_x$ system (solid circles). Data are shown for a resonance frequency, ν , of 12 MHz . It can be seen that the relaxation rate decreases signifi-

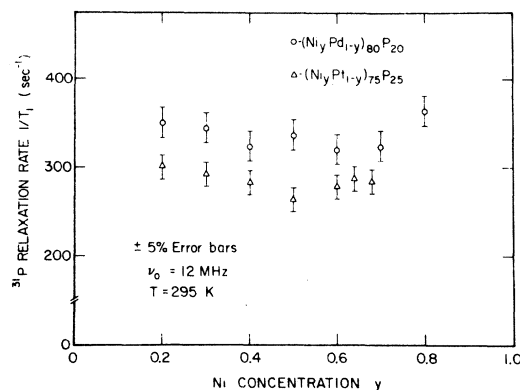


FIG. 2. Room-temperature ^{31}P nuclear spin-lattice relaxation rate vs Ni concentration: open circles— $(\text{Ni}_y\text{Pd}_{1-y})_{80}\text{P}_{20}$; open triangles— $(\text{Ni}_y\text{Pt}_{1-y})_{75}\text{P}_{25}$. $1/T_1$ for ^{31}P is independent of the relative transition-metal composition for these systems.

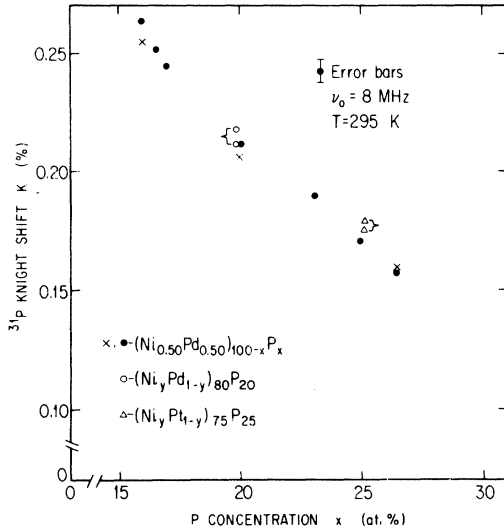


FIG. 3. Room-temperature ^{31}P Knight shift vs P concentration for the $(\text{Ni}_{0.50}\text{Pd}_{0.50})_{100-x}\text{P}_x$ system: solid circles - Ref. 8; crosses - this work. The two open circles with bracket represent the range of values for $(\text{Ni}_y\text{Pd}_{1-y})_{80}\text{P}_{20}$, Ref. 8, while the open triangles with bracket represent the range of values for $(\text{Ni}_y\text{Pt}_{1-y})_{75}\text{P}_{25}$, Ref. 8. K for ^{31}P depends only on the metalloid concentration and not on the relative transition-metal composition for these systems.

cantly as the P concentration increases from $x = 16$ to 26.5. Figure 2 shows the observed ^{31}P relaxation rate at room temperature and 12 MHz as a function of Ni concentration, y , for both $(\text{Ni}_y\text{Pd}_{1-y})_{80}\text{P}_{20}$ and $(\text{Ni}_y\text{Pt}_{1-y})_{75}\text{P}_{25}$ (open circles and open triangles, respectively). In contrast to the behavior for $(\text{Ni}_{0.50}\text{Pd}_{0.50})_{100-x}\text{P}_x$, both $(\text{Ni}_y\text{Pd}_{1-y})_{80}\text{P}_{20}$ and $(\text{Ni}_y\text{Pt}_{1-y})_{75}\text{P}_{25}$ have a relaxation rate which remains unchanged within the error over the entire range of Ni concentration ($y = 0.20$ to 0.80 in the former and $y = 0.20$ to 0.68 in the latter.) This behavior might be expected as a change in the P concentration would vary the average number of electrons per atom, while a change in Ni relative to Pd or Ni relative to Pt would not. It is also important to note that the relaxation rate value characteristic of all the $(\text{Ni}_y\text{Pd}_{1-y})_{80}\text{P}_{20}$ alloys is the same as that for $(\text{Ni}_{0.50}\text{Pd}_{0.50})_{100-x}\text{P}_x$ with $x = 20$. Similarly, the value characteristic of all the $(\text{Ni}_y\text{Pt}_{1-y})_{75}\text{P}_{25}$ alloys falls quite close to that for $(\text{Ni}_{0.50}\text{Pd}_{0.50})_{100-x}\text{P}_x$ with

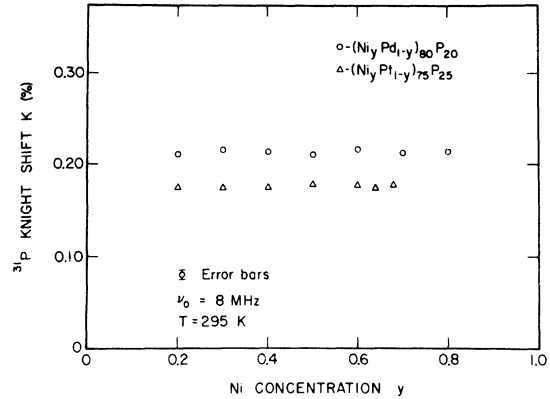


FIG. 4. Room-temperature ^{31}P Knight shift vs Ni concentration: open circles - $(\text{Ni}_y\text{Pd}_{1-y})_{80}\text{P}_{20}$, Ref. 8; open triangles - $(\text{Ni}_y\text{Pt}_{1-y})_{75}\text{P}_{25}$, Ref. 8. K for ^{31}P is independent of the relative transition-metal composition for these systems.

$x = 25$. We have illustrated this point in Fig. 1. The two open circles with bracket at $x = 20$ indicate the range of values obtained for $(\text{Ni}_y\text{Pd}_{1-y})_{80}\text{P}_{20}$, while the open triangles and bracket at $x = 25$ do likewise for $(\text{Ni}_y\text{Pt}_{1-y})_{75}\text{P}_{25}$. Furthermore, this is exactly the same behavior as that observed for the ^{31}P Knight shift in our earlier work. For these same three systems, Figs. 3 and 4 show the dependence of the room-temperature ^{31}P Knight shift (in %), K , as a function of the P concentration, x , and Ni concentration, y , respectively. [The circles and triangles, both open and closed, are data replotted from the earlier work.⁸ However, the Knight-shift values have been corrected by using a later and more accurate value for the ^{31}P salt reference. $\gamma = 1.7236_0$ kHz/Oe was used in this work instead of the original value of $\gamma = 1.7241_4$ kHz/Oe. The Knight-shift measurements in the earlier work were carried out by utilizing a steady-state technique with the Varian wide-line VF-16 cross-coil spectrometer. For comparison, we remeasured the ^{31}P Knight shift for three of the $(\text{Ni}_{0.50}\text{Pd}_{0.50})_{100-x}\text{P}_x$ alloys ($x = 16, 20$, and 26.5) by using the integration of a single pulse free-induction decay as described above. As indicated by the crosses in Fig. 3, the two sets of results are in agreement.] As discussed in detail in Sec. IV, the entire relaxation rate and Knight-shift behavior is consistent with a rigid-band type of behavior and indicates a degree of similarity in the

TABLE I. ^{31}P NMR Knight shift and spin-lattice relaxation rate for $(\text{Ni}_{0.50}\text{Pd}_{0.50})_{100-x}\text{P}_x$ at 4.2, 77, and 295 K.

x	$T = 4.2$ (K)		$T = 77$ (K)		$T = 295$ (K)	
	K (%)	$1/T_1$ (sec $^{-1}$)	K (%)	$1/T_1$ (sec $^{-1}$)	K (%)	$1/T_1$ (sec $^{-1}$)
16.0	0.257 ± 0.005	$6.58 \pm 5\%$	0.247 ± 0.005	$106 \pm 5\%$	0.257 ± 0.005	$446 \pm 5\%$
20.0	0.209 ± 0.005	$4.57 \pm 5\%$	0.201 ± 0.005	$76.9 \pm 5\%$	0.207 ± 0.005	$337 \pm 5\%$
26.5	0.158 ± 0.005	$3.12 \pm 5\%$	0.151 ± 0.005	$50.0 \pm 5\%$	0.158 ± 0.005	$230 \pm 5\%$

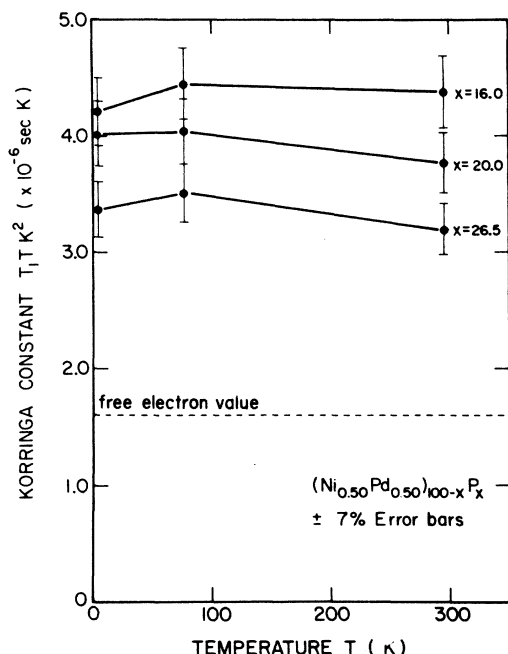


FIG. 5. Experimental Korrington constant vs temperature for the $(\text{Ni}_{0.50}\text{Pd}_{0.50})_{100-x}\text{P}_x$ system. The Korrington constant for completely free s electrons interacting with ^{31}P nuclei is 1.60×10^{-6} sec K. The experimental values are indeed constant with temperature but decrease with metalloid concentration.

electronic structure for all three systems.

For three compositions of the $(\text{Ni}_{0.50}\text{Pd}_{0.50})_{100-x}\text{P}_x$ system, $x = 16, 20,$ and 26.5 , additional pulsed NMR measurements of the ^{31}P relaxation rate and Knight shift were carried out at 77 and 4.2 K. These results, along with the room-temperature values, are summarized in Table I. Figure 5 shows a plot of the experimental Korrington constant (in sec K), T_1TK^2 , versus the temperature (in K), T , for the three alloys. It can be seen that T_1TK^2 is essentially independent of temperature within the error for all three compositions. The values of the experimental Korrington constants are $4.35, 3.94,$ and 3.36×10^{-6} sec K for $x = 16, 20,$ and 26.5 , respectively. The Korrington constant for completely free s electrons interacting with the ^{31}P nuclei is 1.60×10^{-6} sec K. In other words, estimates of T_1 using the measured Knight shifts and Korrington's²⁴ (free s electron) relation are shorter than the experimental ones. These results will be discussed later in Sec. IV in terms of the electronic character at the Fermi surface, and electron-electron interactions.

B. Magnetic susceptibility

Figure 6 shows the measured magnetic susceptibility at room temperature (in emu/mole), $\chi - \chi_{\text{core}}$, as a function of P concentration x , for the $(\text{Ni}_{0.50}\text{Pd}_{0.50})_{100-x}\text{P}_x$

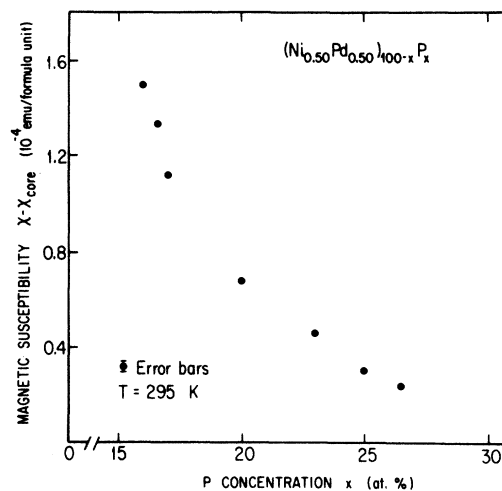


FIG. 6. Corrected room-temperature magnetic susceptibility vs P concentration for the $(\text{Ni}_{0.50}\text{Pd}_{0.50})_{100-x}\text{P}_x$ system. Like $1/T_1$ and K , $\chi - \chi_{\text{core}}$ depends on the metalloid concentration.

system (solid circles). The measured susceptibility values have been corrected for the diamagnetism of the cores. The core contribution for Ni, Pd, and Pt can be estimated from the measured susceptibilities for Cu, Ag, and Au,²⁵ respectively, by subtracting a free-electron estimate for the conduction-electron spin paramagnetism. In each case, the noble metal will have a core very similar to the adjacent transition metal; the one additional electron, however, fills the d band and suppresses the corresponding contribution. The core contributions can also be estimated from the measured diamagnetic susceptibilities of Ni^{2+} , Pd^{2+} , and Pt^{2+} .²⁶ Both methods yield essentially the same results. The core contribution for P is very small and can be estimated

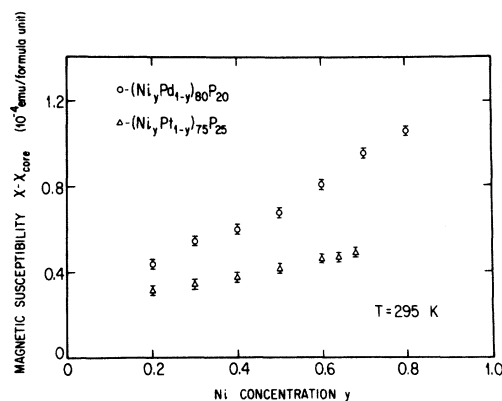


FIG. 7. Corrected room-temperature magnetic susceptibility vs Ni concentration: open circles - $(\text{Ni}_y\text{Pd}_{1-y})_{80}\text{P}_{20}$; open triangles - $(\text{Ni}_y\text{Pt}_{1-y})_{75}\text{P}_{25}$. Unlike $1/T_1$ and K , $\chi - \chi_{\text{core}}$ depends on the relative transition-metal compositions.

TABLE II. Magnetic susceptibility, corrected for core diamagnetism, for $(\text{Ni}_y\text{Pt}_{1-y})_{75}\text{P}_{25}$ at 77 and 295 K.

y	$\chi(77 \text{ K}) - \chi_{\text{core}}$ (10^{-4} emu/mole)	$\chi(295 \text{ K}) - \chi_{\text{core}}$ (10^{-4} emu/mole)
0.20	0.35 ± 0.02	0.31 ± 0.02
0.30	0.37 ± 0.02	0.34 ± 0.02
0.40	0.52 ± 0.02	0.38 ± 0.02
0.50	0.52 ± 0.02	0.42 ± 0.02
0.60	0.57 ± 0.02	0.46 ± 0.02
0.64	0.56 ± 0.02	0.46 ± 0.02
0.68	0.56 ± 0.02	0.49 ± 0.02

from the measured diamagnetic susceptibility of P^{5+} . It can be seen from Fig. 6 that $\chi - \chi_{\text{core}}$ decreases with increasing P concentration as is the case for both the ^{31}P relaxation rate and Knight shift. However, in contrast to the relaxation rate and Knight-shift behavior, $\chi - \chi_{\text{core}}$ decreases quite sharply until $x \approx 20$ and then tails off. This change is interpreted in a rigid-band picture and associated with a change in the density of states at the Fermi energy (see Sec. IV).

Figure 7 shows the measured magnetic susceptibility at room temperature (in emu/mole), $\chi - \chi_{\text{core}}$, as a function of the Ni concentration, y , for both the $(\text{Ni}_y\text{Pd}_{1-y})_{80}\text{P}_{20}$ and $(\text{Ni}_y\text{Pt}_{1-y})_{75}\text{P}_{25}$ systems (open circles and open triangles, respectively). In contrast to the ^{31}P relaxation rate and Knight-shift behavior, $\chi - \chi_{\text{core}}$ increases significantly as the Ni concentration is increased relative to Pd or Pt. Additional measurements were made of $\chi - \chi_{\text{core}}$ at 77 K for the $(\text{Ni}_y\text{Pt}_{1-y})_{75}\text{P}_{25}$ system. These results, along with the room-temperature values, are listed in Table II. We note a small but consistent increase in $\chi - \chi_{\text{core}}$ as the temperature is decreased from room temperature to 77 K. This temperature dependence will be discussed again when we consider the ^{195}Pt Knight-shift results (see Secs. III C and IV).

C. ^{195}Pt NMR Knight shift and spin-lattice relaxation rate

Measurements of the ^{195}Pt Knight shift were made for all seven compositions of $(\text{Ni}_y\text{Pt}_{1-y})_{75}\text{P}_{25}$ at room temperature and three compositions ($y = 0.20, 0.50,$ and 0.68) at 77 K. The results, obtained at 12 MHz, are listed in Table III. [In our earlier work, a preliminary value of $-0.10\% \pm 0.05\%$ was reported for the room-temperature ^{195}Pt Knight shift in $(\text{Ni}_{0.20}\text{Pt}_{0.80})_{75}\text{P}_{25}$, the most Pt-rich composition.⁸ However, problems with filling factor prevented any systematic study of the Pt NMR using the steady-state spectrometer.] We note that the ^{195}Pt Knight shift does depend on the Ni concentration, y , in these systems and

TABLE III. ^{195}Pt NMR Knight shift in $(\text{Ni}_y\text{Pt}_{1-y})_{75}\text{P}_{25}$ at 77 and 295 K.

y	$K(77 \text{ K})$ (%)	$K(295 \text{ K})$ (%)
0.20	-0.07 ± 0.03	$+0.02 \pm 0.03$
0.30	...	-0.06 ± 0.03
0.40	...	-0.06 ± 0.03
0.50	-0.20 ± 0.03	-0.11 ± 0.03
0.60	...	-0.23 ± 0.03
0.64	...	-0.28 ± 0.03
0.68	-0.34 ± 0.03	-0.27 ± 0.03

demonstrates a systematic decrease as the temperature is decreased from room temperature to 77 K. In Sec. IV, these dependences (composition and temperature) will be utilized with corresponding dependences in the magnetic susceptibility in order to quantitatively separate the contributions to the ^{195}Pt Knight shift. We do note, however, that the values for the ^{195}Pt Knight shift in $(\text{Ni}_y\text{Pt}_{1-y})_{75}\text{P}_{25}$ are small in comparison to the value of -3.5% for ^{195}Pt in pure crystalline Pt.²⁷ The large negative Knight shift for ^{195}Pt in Pt metal has been attributed to a dominant core-polarization contribution.²⁸ The resulting positive increase in the Knight shift for ^{195}Pt in the metallic glasses provides strong evidence that the transition-metal d states are being filled which is consistent with a charge transfer from the metalloid to transition-metal atoms. A preliminary measurement of the ^{195}Pt spin-lattice relaxation time, T_1 , for the $(\text{Ni}_{0.20}\text{Pt}_{0.80})_{75}\text{P}_{25}$ composition yielded a room-temperature value of approximately 0.5 msec.

IV. ANALYSIS AND DISCUSSION

In order to understand the observed NMR and magnetic susceptibility behavior, we will employ the customary rigid two-band model.^{29,30} It is assumed that there are two overlapping partially-filled bands, a narrow one associated with the d electrons (localized near the transition-metal sites) and a broad one associated with s and perhaps p electrons (nonlocalized conduction electrons). In general, for transition metals and transition-metal alloys, the NMR Knight shift can be expressed in terms of three contributions

$$K = K_s + K_d + K_0 \quad (1)$$

K_s is the "direct contact shift" resulting from a polarization of the conduction s electrons by the external magnetic field which is communicated to the nuclei via a contact hyperfine interaction. K_0 is the "orbital (or Van Vleck) shift" resulting from a second-order

perturbation effect of the magnetic field whereby higher unoccupied states possessing orbital magnetic moments are mixed into the occupied states giving rise to a temperature-independent contribution. The interpretation of K_d depends on whether we are considering the transition-metal or nontransition-metal constituent in the alloy. For the transition-metal constituent, K_d represents the "core-polarization shift" arising from a polarization of the d electrons by the external magnetic field which is communicated to the transition-metal nuclei via an exchange interaction that perturbs the inner closed-shell s electrons, along with a contact hyperfine interaction. For the nontransition-metal constituent, K_d represents the " d -polarization shift" resulting from a polarization of the transition-metal d electrons by the magnetic field which is communicated to the nontransition-metal nuclei via an s - d exchange interaction that polarizes the conduction s electrons, along with the contact hyperfine interaction. For a transition metal or transition-metal alloy, the magnetic susceptibility can be expressed in terms of its contributions

$$\chi = \chi_s + \chi_d + \chi_L + \chi_{\text{core}} + \chi_0 \quad (2)$$

where χ_s and χ_d are the paramagnetic spin susceptibilities of the s and d bands, respectively, χ_0 is the orbital paramagnetic susceptibility, χ_{core} is the diamagnetic susceptibility of the cores and $\chi_L = -(\frac{1}{3}) \times (m/m^*)^2 \chi_s$ is the Landau diamagnetism. From the discussion above, the three terms in the Knight shift can be related to corresponding terms in the susceptibility and, hence, density of states by

$$K = \alpha_s \chi_s + \alpha_d \chi_d + \alpha_0 \chi_0 \quad (3)$$

$$K = \alpha_s \mu_B^2 N_s(E_F) + \alpha_d \mu_B^2 N_d(E_F) + \alpha_0 \chi_0 \quad (3)$$

where we have used the Pauli expression for the spin susceptibilities. α_s , α_d , and α_0 are the respective electron-nucleus coupling coefficients for the various contributions (they are, of course, different for ^{31}P and ^{195}Pt); $N_s(E_F)$ and $N_d(E_F)$ are the respective densities of states at the Fermi energy for the s and d bands, and μ_B is the Bohr magneton. Similarly, the nuclear spin-lattice relaxation rate for transition-metal alloys can be expressed in terms of such contributions

$$1/T_1 = (1/T_1)_s + (1/T_1)_d + (1/T_1)_0 \quad (4)$$

where the contributions are related to the respective densities of states by

$$1/T_1 = \beta_s [N_s(E_F)]^2 + \beta_d [N_d(E_F)]^2 + \beta_0 [N_d(E_F)]^2 \quad (5)$$

The electron-nucleus coupling coefficients are now β_s , β_d , and β_0 , and T is the temperature. For each band separately, the spin contributions to the Knight

shift and relaxation rate can be related by a Korringa relation (i.e., $1/T_1 T \propto K^2$). This is not the case for the orbital contribution as the orbital relaxation rate depends directly on $N_d(E_F)$, where the orbital shift does not. In general, the orbital contributions are important in situations where there exists narrow, partially filled, non- s bands (i.e., the d band in transition metals and their alloys). However, the contribution does become small when the band is nearly filled (or nearly empty). Such is the case for the Ni-Pd-P and Ni-Pt-P systems and, hence, we will neglect K_0 , $(1/T_1)_0$, and χ_0 .

In Sec. III, we noted that the ^{31}P relaxation rate and Knight shift for the three systems depended only on the P concentration, x , and not on the Ni concentration, y , nor whether the second transition metal was Pd or Pt. On the other hand, the magnetic susceptibility, $\chi - \chi_{\text{core}}$, does depend on the relative transition-metal composition as well as the metalloid concentration. Furthermore, as the P concentration increases from 16 to 26.5, $\chi - \chi_{\text{core}}$ decreases sharply by a factor of 6.3 (with a pronounced kink at $x \approx 20$), while the relaxation rate and Knight shift decrease by factors of 1.9 and 1.6, respectively. We attribute the sharp initial decrease in $\chi - \chi_{\text{core}}$ to a filling of the d band and, hence, a decrease in $N_d(E_F)$ as the P concentration increases. This conclusion is further supported by the ^{195}Pt Knight-shift results. The d band for Ni-Pd-P becomes essentially full at $x \approx 20$. It is interesting to note that if all of the P valence electrons are transferred into the d band, the rigid model predicts that the d band will be filled at a P concentration of 11%. Our results imply that slightly more than half of the P electrons go into the conduction band. Such a conclusion is consistent with the magnetization and Mössbauer studies on some $T_{100-x}M_x$ metallic glasses, where T represents a transition-metal combination of Fe and Ni, and M represents a metalloid combination of B, C, and P.³¹ The behavior of the saturation magnetic moment and isomer shift indicate that metalloids with more sp electrons (e.g., P) donate more electrons to the transition-metal d band. In particular the results suggest that P donates 2.4 electrons per atom to the common d band of T .³¹ In view of the susceptibility behavior, the very systematic behaviors of the ^{31}P relaxation rate and Knight shift indicate that the d terms in both are relatively small compared to the s terms. This is a consequence of the ^{31}P electron-nucleus coupling coefficients α_d and β_d being small. We then have

$$K \approx \alpha_s N_s(E_F), \quad 1/T_1 \approx \beta_s [N_s(E_F)]^2 \quad (6)$$

[Also, the existence of a Korringa relationship between the relaxation rate and Knight shift for ^{31}P in $(\text{Ni}_{0.50}\text{Pd}_{0.50})_{100-x}\text{P}_x$ implies that only one term is important.] Hence, the systematic behavior of the ^{31}P Knight shift and relaxation rate indicate a similarity

in the electronic structure for these systems, in particular the s band and $N_s(E_F)$. The observed reduction in K and $1/T_1$ with increasing P concentration can arise from either a reduction in $N_s(E_F)$ as E_F increases or a reduction in the amount of s character as reflected in α_s and β_s . In view of the discussion above, the experimental values of T_1TK^2 reported for the ^{31}P resonance in Sec. III are a measure of α_s^2/β_s . Also, as indicated earlier, estimates of T_1 using the measured Knight shifts and Korringa's²⁴ relation are shorter than the experimental ones. The discrepancy cannot be due to relaxation processes other than the direct contact interaction since this would cause experimental T_1 's to be shorter than the Korringa values. Such discrepancies are usually attributed to exchange and correlation effects which are neglected in the free-electron estimate.³² In their NMR work on electroplated and chemically deposited $\text{Ni}_{100-x}\text{P}_x$ metallic glasses ($15 \leq x \leq 25$), Bennett *et al.*³³ report a Korringa constant for ^{31}P which is three times the value for pure s electrons. They attribute this to an appreciable exchange enhancement for these materials, indicating substantial d character at the Fermi surface. Furthermore, the $\text{Ni}_{100-x}\text{P}_x$ alloys prepared by the two techniques gave different Knight shifts, suggesting (glassy) local structures with different electronic structures. In contrast to our rapidly quenched Ni-Pd-P and Ni-Pt-P systems, Bennett *et al.*³³ found that both electroplated and chemically deposited $\text{Ni}_{100-x}\text{P}_x$ alloys had a ^{31}P Knight shift which was essentially independent of composition for $x \geq 19$.

Unlike the ^{31}P Knight shift, the ^{195}Pt Knight shift for the $(\text{Ni}_y\text{Pt}_{1-y})_{75}\text{P}_{25}$ system does depend on the Ni concentration, y . This dependence is utilized to separate the ^{195}Pt Knight shift into its s and d contributions; both are now significant. The procedure is similar to that employed by Clogston *et al.*²⁸ for crystalline Pt and Pd. The composition dependences of the ^{195}Pt Knight shift $K(y)$ and magnetic susceptibility $\chi(y) - \chi_{\text{core}}(y)$ enter through the d term. If we eliminate $\chi_d(y)$ between the Knight shift Eq. (1) and susceptibility Eq. (2), and use $\chi_L = -(\frac{1}{3})(m/m^*)^2 \times \chi_s$, we obtain

$$K(y) = \alpha_d[\chi(y) - \chi_{\text{core}}(y)] + [(\alpha_s - \alpha_d) + (\frac{1}{3})(m/m^*)^2 \alpha_d] \chi_s \quad (7)$$

A plot of $K(y)$ versus $\chi(y) - \chi_{\text{core}}(y)$, using the Ni concentration y as an implicit parameter, yields a straight line whose slope is the electron-nucleus coefficient, or hyperfine coupling constant, α_d , for ^{195}Pt . This is shown in Fig. 8, where we find a value of $\alpha_d = -0.16 \times 10^3$ mole/emu [or a hyperfine field per μ_B of d spin, $H_{\text{hr}}(d)$, equal to -910 kOe/ μ_B]. The corresponding value for ^{195}Pt in pure crystalline Pt is -1200 kOe/ μ_B .²⁸ Furthermore, we note that any temperature dependence for the ^{195}Pt Knight shift

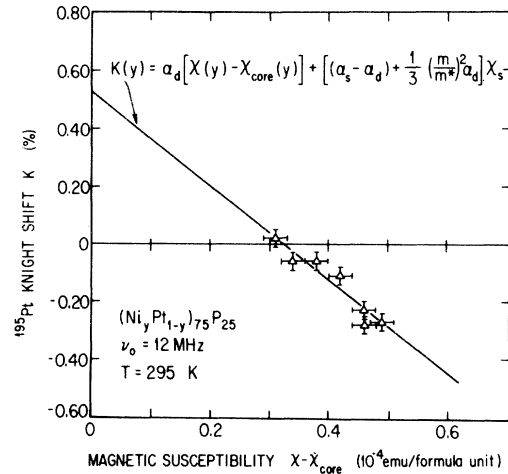


FIG. 8. Room-temperature ^{195}Pt Knight shift vs magnetic susceptibility for the $(\text{Ni}_y\text{Pt}_{1-y})_{75}\text{P}_{25}$ system. The straight line is the best fit to the data and enables a decomposition of K and $\chi - \chi_{\text{core}}$ into their s - and d -band contributions.

would enter principally through the d term. Again, we can write

$$K(T) = \alpha_d[\chi(T) - \chi_{\text{core}}] + [(\alpha_s - \alpha_d) + (\frac{1}{3})(m/m^*)^2 \alpha_d] \chi_s \quad (8)$$

and plot the Knight shift versus a magnetic susceptibility using temperature as the implicit parameter. The observed temperature dependences for the ^{195}Pt Knight shift (Table III) and magnetic susceptibility (Table II) yield values of α_d which are consistent with the result reported above. Estimates for α_s (for ^{195}Pt), $N_s(E_F)$, and $N_d(E_F)$ are obtained by using the Pauli form for the spin paramagnetism [$\chi = \mu_B^2 N(E_F)$] and treating the conduction (s and p) electrons as free with an effective mass $m^* \approx m$ the electron mass; i.e., in emu/mole,

$$\chi = 1.86 \times 10^{-6} (M/\rho)^{2/3} (n_s)^{1/3} \quad (9)$$

In the above form, M is the atomic mass, ρ is the density, and n_s is the number of conduction electrons per atom. For $(\text{Ni}_{0.50}\text{Pt}_{0.50})_{75}\text{P}_{25}$, $(M/\rho) = 8.73$ cm³/mole. By taking $n_s = 1.3$ conduction electrons per atom, we obtain $\chi_s = 8.6 \times 10^6$ emu/mole and $N_s(E_F) = 1.2 \times 10^{34}$ /erg cm³. The estimate for n_s comes from the electrical resistivity and x-ray diffraction work of Sinha.⁶ Substituting the above value for χ_s into the expression for the y intercept from Fig. 8 [Eq. (7)], along with $m^* \approx m$ and $\alpha_d = -1.6 \times 10^3$ mole/emu, we obtain $\alpha_s = +0.50 \times 10^3$ mole/emu. This is equivalent to a hyperfine field per μ_B of s spin, $H_{\text{hr}}(s)$, equal to $+5200$ kOe/ μ_B . The corresponding value for ^{195}Pt in pure crystalline Pt metal is $+12000$ kOe/ μ_B .²⁸ Subtracting $\frac{2}{3}\chi_s$ from $\chi - \chi_{\text{core}}$ gives $\chi_d = 36 \times 10^{-6}$ emu/mole (χ_0 being neglected). Assuming the Pauli expression for χ_d yields $N_d(E_F) = 4.8 \times 10^{34}$ /erg cm³.

V. CONCLUSIONS

From the NMR and magnetic susceptibility work, we can draw the following conclusions about the Ni-Pd-P and Ni-Pt-P systems in particular, with implications for the $T_{100-x}M_x$ metallic glasses in general.

(1) The ^{31}P Knight shift and relaxation rate for both systems depend only on the P concentration, x , and not the Ni concentration, y , nor whether the second transition metal is Pd or Pt. (2) The ^{31}P Knight shift and relaxation rate for both systems are attributed solely to the direct contact hyperfine interaction, with the d -polarization contribution [i.e., $\alpha_d(^{31}\text{P})$ and $\beta_d(^{31}\text{P})$] being negligible. (3) The results can be described by a rigid two-band model; a narrow one associated with the d electrons (localized at the transition-metal sites) and an overlapping broad band associated with the s and perhaps p electrons. (4) The two systems have a similar electronic structure, in particular the s band and $N_s(E)$. The magnetic susceptibility provides a "mapping" of the total density of states. (5) Consistent with the DRP model,⁹ there is evidence of a transfer of charge from the P metalloid atoms to the transition-metal d states in both Ni-Pd-P and Ni-Pt-P. For Ni-Pd-P, these states become full for $x \approx 20$. Since the rigid-band model predicts that if all of the P electrons go into the d states, the filling would be complete for $x \approx 11$, we conclude that slightly more than half of the P electrons go into the conduction band. (6) There is no evidence of any minimum in the density of states as predicted by the Nagel and Tauc theory.¹⁵ (7) The various ^{31}P Knight-shift and relaxation rate values satisfy Korringa relationships, with the value of

T_1TK^2 decreasing as the P concentration increases. The values of T_1TK^2 range from two to three times the free-electron value. (8) The ^{195}Pt Knight shift in Ni-Pt-P has contributions from both the direct contact hyperfine interaction and core polarization (the orbital contribution being negligible). Plots of the ^{195}Pt Knight shift versus magnetic susceptibility, using both the composition and temperature as implicit parameters, yield values for the electron-nucleus hyperfine coupling constants of $\alpha_s(^{195}\text{Pt}) = +0.50 \times 10^3$ mole/emu ($+5200$ kOe per μ_B of s spin) and $\alpha_d(^{195}\text{Pt}) = -0.16 \times 10^3$ mole/emu (-910 kOe per μ_B of d spin). [By assuming the Pauli form for both the s - and d -band paramagnetic susceptibilities and treating the s -band conduction electrons as free, one obtains estimates for $N_s(E_F)$ and $N_d(E_F)$ from the susceptibility measurements.]

ACKNOWLEDGMENTS

One of us (W.A.H.) would like to express his deep appreciation to the Solid State Group, U.C.L.A., for the kind hospitality extended to him during his sabbatic leave visit. The pulsed NMR work at U.C.L.A. was supported by the NSF under Grant No. DMR 77-23577 and the UCLA Academic Senate Research Committee. The magnetic susceptibility work at the University of Connecticut was supported both by the AFOSR under Grant No. AFOSR 80-0030 and the University of Connecticut Research Foundation. Sample preparation and characterization at the California Institute of Technology was supported by the ERDA under Contract No. AT(04-3)-822.

*On leave from: Department of Physics and Institute of Materials Science, University of Connecticut, Storrs, Connecticut 06268.

†Permanent address: Naval Surface Weapons Center, White Oak, Silver Spring, Maryland 20910.

¹J. J. Gilman, *Phys. Today* **28**, 46 (1975).

²P. L. Maitrepierre, *J. Appl. Phys.* **40**, 4826 (1969).

³J. Dixmier and P. Duwez, *J. Appl. Phys.* **44**, 1189 (1973).

⁴A. K. Sinha and P. Duwez, *J. Phys. Chem. Solids* **32**, 267 (1971).

⁵B. Y. Boucher, *J. Non-Cryst. Solids* **7**, 277 (1972).

⁶A. K. Sinha, *Phys. Rev. B* **1**, 4541 (1970).

⁷H. S. Chen, *Acta Metall.* **22**, 1505 (1974).

⁸W. A. Hines, L. T. Kabacoff, R. Hasegawa, and P. Duwez, *J. Appl. Phys.* **49**, 1724 (1978).

⁹D. E. Polk, *Scr. Metall.* **4**, 117 (1970).

¹⁰J. D. Bernal, *Nature* **185**, 68 (1960).

¹¹S. R. Nagel, *Scr. Metall.* **12**, 43 (1978).

¹²A. Bienenstock and B. G. Bagley, *J. Appl. Phys.* **37**, 4840 (1966).

¹³H. S. Chen and B. K. Park, *Acta Metall.* **21**, 395 (1973).

¹⁴S. R. Nagel, G. B. Fisher, J. Tauc, and B. G. Bagley, *Phys.*

Rev. B **13**, 3284 (1976).

¹⁵S. R. Nagel and J. Tauc, *Phys. Rev. Lett.* **35**, 380 (1975).

¹⁶J. M. Ziman, *Philos. Mag.* **6**, 1013 (1961).

¹⁷R. Evans, D. A. Greenwood, and P. Lloyd, *Phys. Lett. A* **35**, 57 (1971).

¹⁸P. J. Cote, *Solid State Commun.* **18**, 1311 (1976).

¹⁹J. L. Beebe, *Phys. Rev.* **141**, 781 (1966).

²⁰P. Duwez, in *Techniques of Metal Research*, edited by R. F. Bunshah (Interscience, New York, 1968), Vol. I, part 1, Chap. 7, p. 347.

²¹W. G. Clark, *Rev. Sci. Instrum.* **35**, 316 (1964); J. A. McNeil and W. G. Clark, *Rev. Sci. Instrum.* **44**, 844 (1973); J. A. McNeil and W. G. Clark, *Proceedings of the 1st Specialized Colloque Ampere on Pulsed Nuclear Magnetic Resonance and Spin Dynamics in Solids, Krakow, Poland, 1973*, edited by J. W. Hennel (Institute of Nuclear Physics, Krakow, Poland, 1973).

²²Varian Associates, NMR Chart of the Nuclei.

²³S. Foner, *Rev. Sci. Instrum.* **30**, 548 (1959).

²⁴J. Korringa, *Physica (Utrecht)* **16**, 601 (1950).

²⁵P. W. Selwood, *Magnetochemistry* (Interscience, New York, 1956), pp. 355-364.

²⁶See Ref. 25 (p. 78).

²⁷T. J. Rowland, *J. Phys. Chem. Solids* 7, 95 (1958).

²⁸A. M. Clogston, V. Jaccarino, and Y. Yafet, *Phys. Rev.* 134, A650 (1964).

²⁹L. E. Drain, *Metall. Rev.* 12, 195 (1967).

³⁰L. H. Bennett, R. E. Watson, and G. C. Carter, *J. Res. Nat. Bur. Stand. Sect. A* 74, 569 (1970).

³¹R. Hasegawa, R. C. O'Handley, and L. I. Mendelsohn, in

Magnetism and Magnetic Materials, edited by J. J. Becker and G. H. Lander, AIP Conf. Proc. No. 34 (AIP, New York, 1976), p. 298.

³²D. Pines, in *Solid State Physics*, edited by F. Seitz and D. Turnbull (Academic, New York, 1956), Vol. 1, p. 367.

³³L. H. Bennett, H. E. Schone, and P. Gustafson, *Phys. Rev. B* 18, 2027 (1978).